Soft Matter

PAPER

View Article Online
View Journal | View Issue

Cite this: *Soft Matter*, 2015, 11, 8599

Why does high pressure destroy co-non-solvency of PNIPAm in aqueous methanol?

Tiago E. de Oliveira,[ab] Paulo A. Netz,[ab] Debashish Mukherji*[a] and Kurt Kremer*[a]

Received 17th July 2015,
Accepted 26th August 2015

DOI: 10.1039/c5sm01772f

www.rsc.org/softmatter

It is well known that poly(*N*-isopropylacrylamide) (PNIPAm) exhibits an interesting, yet puzzling, phenomenon of co-non-solvency. Co-non-solvency occurs when two competing good solvents for PNIPAm, such as water and alcohol, are mixed together. As a result, the same PNIPAm collapses within intermediate mixing ratios. This complex conformational transition is driven by preferential binding of methanol with PNIPAm. Interestingly, co-non-solvency can be destroyed when applying high hydrostatic pressures. In this work, using a large scale molecular dynamics simulation employing high pressures, we propose a microscopic picture behind the suppression of the co-non-solvency phenomenon. Based on thermodynamic and structural analysis, our results suggest that the preferential binding of methanol with PNIPAm gets partially lost at high pressures, making the background fluid reasonably homogeneous for the polymer. This is consistent with the hypothesis that the co-non-solvency phenomenon is driven by preferential binding and is not based on depletion effects.

1 Introduction

Poly(*N*-isopropylacrylamide) (PNIPAm) is a so-called smart polymer that responds to a wide range of external stimuli, such as temperature, cosolvents, ionic strengths, and pressures. One of the most fascinating and puzzling phenomena of PNIPAm is its ability to exhibit co-non-solvency.[1–7] When a sample of PNIPAm is dissolved in mixtures of water and alcohol under ambient conditions, it collapses when the composition of solvent mixtures is between 5–40% of alcohol concentration.[1–4] Understanding this complex structural transition is not only scientifically challenging,[6,7] but also has a wide variety of applicabilities that range from physics to biology.[8–10] In this context, it has been recently shown that the co-non-solvency can only be explained by the preferential binding of one of the cosolvent components with the polymer. In other words, the competitive displacement of cosolvent components plays a significant role in describing co-non-solvency.[7,11] It was suggested that when a very small amount of better cosolvent is added into the dilute aqueous polymer solution, these better cosolvents bind two monomers potentially far along the backbone forming segmental loops. This loop formation initiates the process leading to a final well collapsed structure of the polymer. Interestingly, this preferential cosolvent binding can also explain the reopening of the polymers at high cosolvent concentrations by the complete decoration of the polymer with cosolvents.[7,11]

Another surprising phenomenon of PNIPAm is when it is exposed to high hydrostatic pressures. It was experimentally observed that when a collapsed PNIPAm between 5–40% of alcohol concentration is kept under high hydrostatic pressures at 298 K, co-non-solvency gets completely destroyed. As a consequence, a PNIPAm chain only remains in the expanded coil state, irrespective of the water–methanol mixing concentrations.[12] The present work is the first attempt to give a detailed microscopic picture of this interesting pressure induced reopening of PNIPAm under co-non-solvency conditions. We use large scale molecular dynamics simulations to study the conformational transition of PNIPAm in aqueous methanol by employing high hydrostatic pressures. We perform thermodynamic and structural analysis to propose a microscopic origin of this high pressure effect.

The remainder of this paper is organized as follows: in Section 2 we briefly state the methodology for simulations and Section 3 presents Results and discussion. Finally we draw our conclusions in Section 4.

2 Simulation method and model

In this study we employ all atom molecular dynamics simulations using GROMACS package.[13] We use the Gromos96 force field[14] for methanol and the SPC/E water model[15] and the force field parameters for PNIPAm are taken from ref. 3. The temperature is set to 298 K using a Berendsen thermostat with a coupling constant of 0.1 ps. The time step for the simulations is chosen as 1 fs. Unless stated otherwise results are shown for the ambient

[a] *Max-Planck Institut für Polymerforschung, Ackermannweg 10, 55128 Mainz, Germany. E-mail: mukherji@mpip-mainz.mpg.de, kremer@mpip-mainz.mpg.de*
[b] *Universidade Federal do Rio Grande do Sul, Porto Alegre, Brazil*

and 500 MPa pressures. However, in some cases, we have also performed simulations at 100 MPa and 200 MPa to systematically test the pressure effects. It should be noted that the all atom force field used here has reasonably good transferability over a wide range of pressures and temperatures.[16] The pressure coupling is done using a Berendsen barostat[17] with a coupling time of 0.5 ps. The electrostatics are treated using Particle Mesh Ewald.[18] The interaction cutoff is chosen as 1.4 nm.

We use a PNIPAm chain of length N = 32 solvated in a simulation box consisting of 2×10^4 solvent molecules at 25% methanol molar concentration x_m, *i.e.* 0.5×10^4 methanol and 1.5×10^4 water molecules, respectively. In some cases, we have also performed simulations over the full concentration range of methanol, ranging from pure water $x_m = 0.0$ to pure methanol $x_m = 1.0$. This system size is large enough to maintain the solvent equilibrium between the local region within the vicinity of the polymer and the bulk aqueous methanol solution. Note that maintaining the solvent equilibrium in molecular simulations is a paramount task, which is most severe when the polymer collapse and expansion are driven by strong local concentration fluctuations of different solvent components. This can either be achieved by using a grand-canonical-like approach[6] or by using a large simulation box.[19] Mid-sized simulation domains are prone to system size effects and, therefore, may lead to unphysical structural fluctuations. Every initial configuration is equilibrated for 50 ns under ambient pressure. The production runs are performed for 450 ns at 298 K and varying pressures. During the production run observables such as end-to-end distance R_{ee}, pair distribution function $g_{ij}(r)$, Kirkwood–Buff integral G_{ij} and potential of mean force $V_{\mathrm{PMF}}(r)$ are calculated. The time scale of simulation used here is approximately one order of magnitude larger than the conformational relaxation time of a PNIPAm chain, which is estimated by calculating the end-to-end autocorrelation function $\langle R_{ee}(t) \cdot R_{ee}(0) \rangle$.

3 Results and discussion

3.1 Polymer conformation under high pressures

We start our discussion by presenting the central result of this paper, which is the structure of the polymer at high pressures. The initial configurations are generated by performing a simulation starting from a completely extended PNIPAm structure at 298 K temperature and ambient pressure. In Fig. 1(a) the green curve (for $t < 50$ ns) presents the time evolution of polymer end-to-end distance R_{ee} during equilibration. The structure collapses within 25 ns of MD run. Then we further monitor the collapsed structure for another 25 ns to identify any unphysical fluctuations, which showed a rather stable collapsed conformation. The last frame of this initially equilibrated sample was used for the production runs under high pressures. The blue curve in Fig. 1(a) presents the time evolution of R_{ee} at 500 MPa calculated over a 450 ns simulation trajectory. It can be appreciated that the polymer remains within a completely globular state for almost 100 ns, with a distinctly prominent stable polymer loop

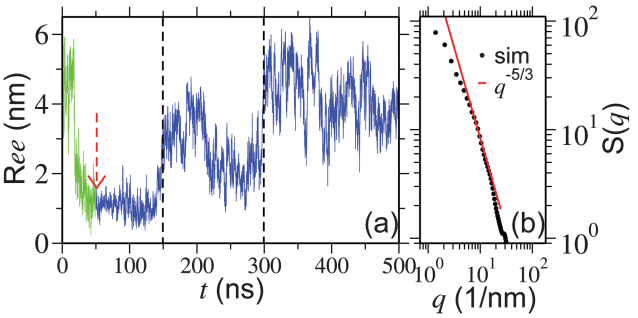

Fig. 1 Part (a) shows the time evolution of polymer end-to-end distance R_{ee}. The results are shown for a chain length N_l = 32 and at a methanol concentration of 25%. Initial equilibration starts with a completely extended configuration of PNIPAm at a temperature of 298 K and ambient pressure (represented by the green curve). A pressure of 500 MPa is employed beginning at 50 ns (represented by the red arrow). Two vertical dashed lines are drawn to present different time regimes during polymer reopening. Between 50 ns $< t <$ 150 ns the polymer remains fully collapsed, for 150 ns $< t <$ 300 ns the end loops get opened and finally the polymer completely opens up for $t >$ 300 ns. Part (b) presents the static structure factor $S(q)$ of a PNIPAm backbone for $t >$ 300 ns. Note that for the calculation of $S(q)$ only alkane backbone was considered.

(see simulation snapshots in Fig. 2). The first expansion occurs at around 150 ns when the end loop opens up. The complete opening of the polymer chain occurs for $t >$ 300 ns. A sequence of simulation snapshots is presented in Fig. 2. Thus our simulations could correctly capture the features observed in the high pressure experiments.[12]

Furthermore, to confirm that we are indeed getting a well extended structure at 500 MPa, we look into the scaling law of the static structure factor for a PNIPAm chain at 500 MPa, which should support the scaling law $S(q) \sim q^{-1/\nu}$ with $\nu = 3/5$ being the Flory exponent.[20,21] In Fig. 1(b) we show $S(q)$ for a

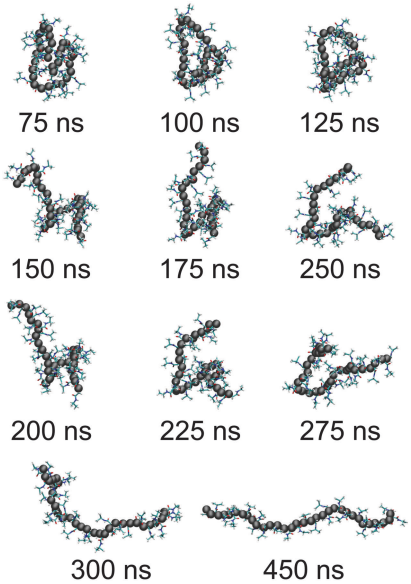

Fig. 2 Sequence of snapshots for a PNIPAm chain of length N_l = 32 at different times as measured during the simulations. To better represent the polymer conformation, we render the alkane backbone with spheres.

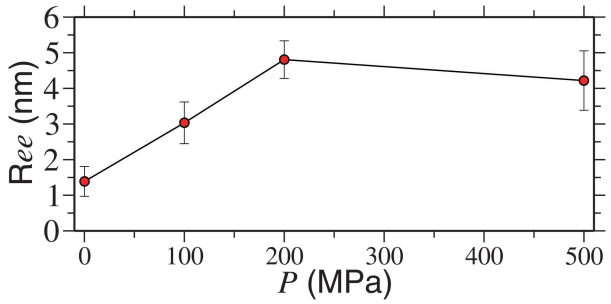

Fig. 3 Polymer end-to-end distance R_{ee} as a function of applied pressure P for a PNIPAm chain of length N_l = 32 and at a temperature of 298 K.

PNIPAm chain at 500 MPa and calculated from the MD trajectory for $t > 300$ ns. Indeed, the data in the range 4 nm^{-1} < q < 20 nm^{-1} can be reasonably well described by a scaling exponent $\nu = 5/3$ known from the self avoiding random walk.[20,21] This range falls within the length scale of 1.6 nm and 0.4 nm. Considering that the gyration radius $R_g \sim 1.7$ nm, the observed length scale is satisfactory. Moreover, it should also be mentioned that ideally a good estimate of $S(q)$ requires long chains and here we are simulating a rather short chain of N_l = 32 (or approximately 10 persistence lengths). Therefore, while the data in Fig. 1(b) are certainly not good enough to derive an apparent exponent, it is reasonable to clearly mark an extended chain.

Here, we also want to comment on the range of pressures used here and in the experiments.[12] It should be noted that a pressure of upto 200 MPa was used in ref. 12. However, thus far, we have only presented results for 500 MPa. Therefore, in Fig. 3 we show a systematic dependence of R_{ee} on pressure. It can be appreciated that the polymer reaches a fully extended state (represented by $R_{ee} \sim 4.5$) at $P \geq 200$ MPa. This gives a very good comparison with the experimental results. For P = 100 MPa, however, we find a semi-collapsed structure (with $R_{ee} \sim 3.0$) for up to 450 ns, the typical simulation time scale investigated here.

The observed prominent loops (see Fig. 2) in our all atom simulations are reminiscent of the proposed mechanism of polymer collapse transition in mixed good solvents.[7] It is known that the loops are formed because of the bridging methanol molecules that can bind two distinctly far monomers along the backbone.[7] Therefore, if the bridging is getting destroyed at high pressures, then there must also be a disruption of methanol–polymer interaction to facilitate the opening of a PNIPAm chain. Therefore, to establish a microscopic picture of the high pressure effects, we first look into the structure of water and methanol within the solvation volume of the polymer.

3.2 Coordination and excess coordination numbers

In this section we perform structural analysis of the polymer solution. For this purpose we calculate the radial distribution function $g_{ij}(r)$ between solution components. To obtain better convergence in $g_{ij}(r)$, we have simulated a single monomer of PNIPAm (represented as NIPAm) in a 25% methanol–water mixture. In Fig. 4 we present NIPAm–methanol and NIPAm–water $g_{ij}(r)$ for

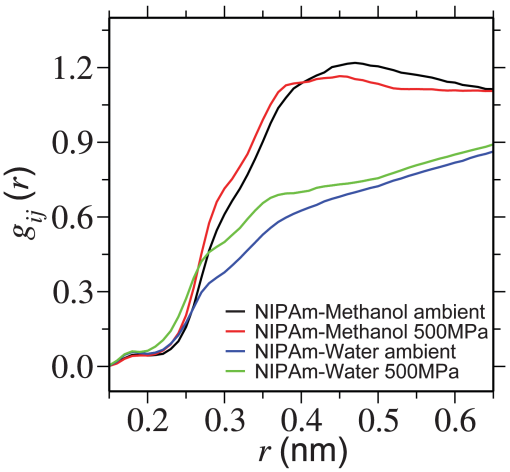

Fig. 4 Radial distribution function $g_{ij}(r)$ showing NIPAm–methanol and NIPAm–water coordination for two different pressures. Simulations are performed at a temperature of 298 K.

two different pressures. It is apparent from the plot that – while methanol coordination reduces partially within the first solvation shell (at around 0.5 nm), the coordination of water increases. This suggests that methanol is getting partially replaced by water within the solvation shell of PNIPAm.

Furthermore, in Table 1 we present an estimate of the change in the coordination number between NIPAm and bulk solution components. It can be appreciated that with increasing pressure the coordination number of NIPAm–methanol only increases by about 16%, whereas NIPAm–water increases by 54%. This suggests that water is replacing methanol in the solvation shell, making the background fluid more homogeneous for the polymers. This is consistent with the expanded structure of the polymer.

The density of the system increases about 15% when the system goes from ambient pressure to 500 MPa. It is known that this increase in density leads to a substantial increase of the average coordination number of water,[22] and also to an increase in the diffusion coefficient at low temperatures,[23] but at high temperatures the effect of the pressure on the diffusion coefficient is the opposite. Indeed, when the high pressure is applied, the diffusion coefficient of water and methanol (data not shown) decreases by about 40% and 50%, respectively. Thus suggesting that the pressure-induced replacement of methanol with water has a thermodynamic rather than a kinetic origin.

A theory that perhaps best connects the relative intermolecular affinity and the solution thermodynamics is the fluctuation theory

Table 1 Various solute–solvent pairs with their respective coordination calculated using $n = 4\pi\int_0^{0.5} g_{ij}(r)r^2\,dr$, bulk solution number density of solution components ρ and the coordination numbers $n\rho$

Pairs at different pressures	n (nm^3)	ρ (nm^{-3})	$n\rho$
NIPAm–methanol ambient	0.4718	6.7749	3.1964
NIPAm–methanol 500 MPa	0.4758	7.8068	3.7145
NIPAm–water ambient	0.2352	20.3248	4.7804
NIPAm–water 500 MPa	0.3123	23.4204	7.3142

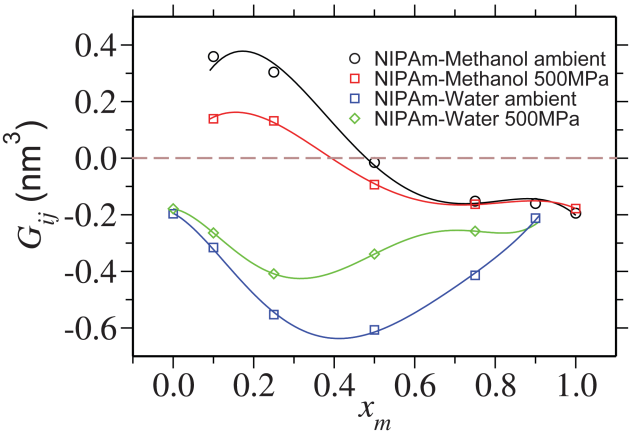

Fig. 5 Kirkwood–Buff integral G_{ij} showing NIPAm–methanol G_{pm} and NIPAm–water G_{pw} excess coordination as a function of methanol molar fraction x_m. Lines are the polynomial fits to the data that are drawn to guide the eye. For pure solvent at x_m = 0.0 and pure cosolvent at x_m = 1.0, individual coordinations G_{pm} and G_{pw} are undefined, respectively. A horizontal dashed line is drawn to show G_{ij} = 0. The data corresponding to the ambient pressure are taken from ref. 6.

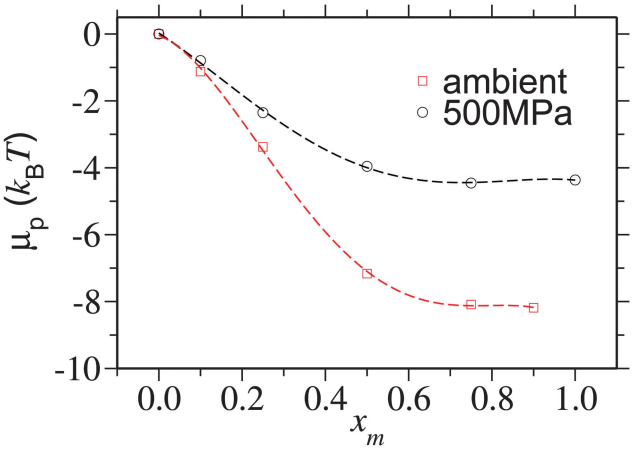

Fig. 6 Chemical potential shift per monomer μ_p/N_l as a function of methanol mole fraction x_m for two different pressures. μ_p is calculated by integrating the data obtained from eqn (2). The data corresponding to the ambient pressure are taken from ref. 6.

of Kirkwood and Buff (KB).[24] KB theory connects $g_{ij}(r)$ to the thermodynamic properties of solutions using the "so called" KB integrals or excess coordinations,

$$G_{ij} = 4\pi\int_0^\infty \left[g_{ij}(r) - 1\right] r^2\, \mathrm{d}r. \qquad (1)$$

In Fig. 5 we summarize NIPAm–methanol G_{pm} and NIPAm–water G_{pw} excess coordination over the full molar concentration range of methanol x_m. Ideally G_{ij} should be taken from the plateau at $r \to \infty$. Moreover, we estimate G_{ij} values by taking averages between 0.9 nm $< r <$ 1.5 nm. Note that the typical correlation lengths in these systems are of the order of 1.5 nm. It can be seen that – in comparison to NIPAm–water excess coordination, NIPAm–methanol still shows preferentiability even at 500 MPa. However, it is reduced by a factor of two. It is interesting to observe that the polymer opens up even when there remains preferentiability. In this context, it is still important to mention that the fully collapsed structure needs a certain fraction of methanol molecules within the solvation volume. Reduction in this fraction may not lead to a well collapsed conformation. Instead, occasionally, one expects to observe a fluctuation in the extended polymer conformations, where instantaneous bridging may occur (forming loops) due to a small fraction of methanol molecules within the solvation shell of PNIPAm.

To better quantify this reduced preferentiability one can translate the information presented in Fig. 5 into chemical potential of PNIPAm μ_p, which can be calculated using,[25]

$$\frac{1}{k_B T}\left(\frac{\partial \mu_p}{\partial \rho_m}\right)_{p,T} = \frac{G_{pw} - G_{pm}}{1 - \rho_m (G_{mw} - G_{mm})}, \qquad (2)$$

where ρ_m is the methanol number density and k_B is the Boltzmann constant. In Fig. 6 we show μ_p as a function of x_m for different N_l's, calculated by integrating eqn (2). For 500 MPa, it can be appreciated that the difference in μ_p between NIPAm in pure methanol (or x_m = 1.0) and NIPAm in pure water (or x_m = 0.0) is reduced to $4k_BT$, which is otherwise $8k_BT$ under the ambient conditions. Thus clearly indicating that by adding methanol molecules into the solution, the solvent quality is not getting as better as in the case of ambient pressure. Note that the methanol driven collapse of PNIPAm under ambient conditions occurs when the solvent quality remains good or even gets increasingly better[6,7] and that this assymetry should be of the order of 8–10k_BT. To further investigate the thermodynamic origin of this reduced preferentiability we also calculate the potential of mean force in the next section.

It is yet important to mention that the polymer collapse can either be initiated by: (a) the bridging and looping scenario presented earlier[6] or (b) the depletion effects.[26] Our arguments of polymer collapse-swelling transition are based on the scenario (a). However, it could also be argued that the depletion effects,[26] that are responsible for polymer collapse under the poor solvent conditions, may be a factor behind PNIPAm collapse in aqueous methanol mixtures under ambient pressure. However, it should be noted that when two competing good solvents are mixed together, such that the dissolved polymer collapses within the intermediate mixing ratios, the collapse occurs when the solvent quality remains good or even gets increasingly better by the addition of better cosolvent (in this case methanol).[6] This makes the polymer conformation decoupled from the solvent quality. Therefore, precluding any explanation based on the depletion effects that can "only" explain poor solvent collapse. Furthermore, the depletion induced attractions can only be enhanced when increasing density. Note that for 500 MPa pressure bulk solution density increases by 15%. Therefore, if the pure depletion effects were the microscopic origin of co-non-solvency, PNIPAm would never open under the influence of higher pressures. The same argument also holds to explain the reopening of PNIPAm at high methanol concentrations. Further suggesting that the bridging scenario seems to be the only possible explanation to co-non-solvency[6,7,11] and pressure induced reopening presented in this work.

3.3 Potential of mean force

Finally we want to study the thermodynamic origin of this interesting conformational transition. For this purpose we have calculated the potential of mean force (PMF) between solute and solvent components. The PMF is calculated using the umbrella sampling[27] over a series of independent simulations at 298 K temperature and 500 MPa pressure, each for a 10 ns long trajectory. The center-of-mass positions between the NIPAm monomer and the solvent components are generated by pulling the solvent component towards the NIPAm monomer using a steered molecular dynamics algorithm. Here the spring constant is chosen as 1000 kJ mol^{-1} nm^{-2} and a velocity of pull was selected as 0.001 nm ps^{-1}. Between 0 and 1.65 nm we choose 120 positions that are constrained using a LINCS algorithm.[28] The PMF is calculated by integrating the constraining forces f_c using the expression,[29,30]

$$V_{\mathrm{PMF}}(r) = \int_{r_0}^{r} \left[\langle f_c \rangle_s + \frac{2k_B T}{s} \right] \mathrm{d}s + \mathrm{const.} \qquad (3)$$

Here $\langle f_c \rangle_s$ is the average force at a distance s between the NIPAm and respective solvent component. r_0 represents the closest proximity that the solvent can approach a NIPAm monomer. The factor $2k_BT/s$ is the entropic correction. The constant term is taken such that the potential goes asymptotically to zero at 1.4 nm.

In Fig. 7 we show $V_{\mathrm{PMF}}(r)$. Looking into the plot under ambient pressure, it becomes apparent that there exists an attractive well for NIPAm–methanol interaction (represented by the black curve), whereas NIPAm–water interaction is repulsive (represented by the blue curve). Furthermore, when the high pressure is applied the attractive well of NIPAm–methanol interaction becomes shallower, indicating a reduced attractive interacting strength between NIPAm and methanol at high pressure. On the other hand NIPAm–water develops a attractive well. The applied pressure, therefore, could decrease the preferentiability of NIPAm–methanol interaction and, at the same time, enhance the NIPAm–water coordination, leading to polymer swelling.

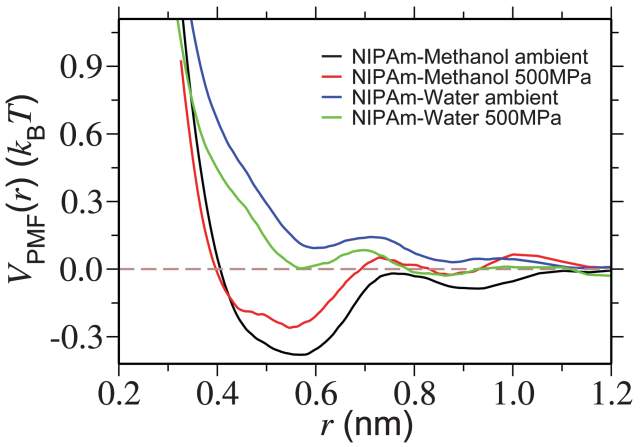

Fig. 7 Potential of mean force $V_{\mathrm{PMF}}(r)$ showing NIPAm–methanol and NIPAm–water interaction strengths for two different pressures. Simulations are performed at a temperature of 298 K.

4 Conclusions

Using molecular dynamics simulations of an all atom model, we unveil the microscopic origin why the application of high hydrostatic pressures can destroy the co-non-solvency phenomenon of poly(*N*-isopropylacrylamide) (PNIPAm) in aqueous methanol mixtures.[12] Performing structural and thermodynamic analysis, we propose that the reopening of a collapsed PNIPAm at 25% methanol concentration is due to the partial loss of preferential binding of methanol with PNIPAm at high pressures, which is the only key factor behind the polymer collapse in a mixture of two competing good solvents.[7] This reduced preferentiability makes the background fluid reasonably homogeneous for PNIPAm. This is consistent with the swollen structure of the polymer under high pressures. Additionally, the results presented here eliminate any possible explanation of the co-non-solvency effect based on pure entropic effects. Had the collapse-swelling transition been dictated by depletion forces, polymer would have never open up under high pressures, especially because depletion forces are most severe under high pressures.

Acknowledgements

The development of this work would not have been possible without fruitful collaboration with Carlos Marques, we take this opportunity to gratefully acknowledge. We thank Walter Richtering for bringing ref. 12 to our attention and Davide Donadio and Torsten Stuehn for many stimulating discussions. T.E.O. and P.A.N. acknowledge financial support from CNPq and CAPES from Brazilian Government and hospitality at the Max-Planck Institut für Polymerforschung, where this work was performed. We thank Robinson Cortes-Huerto and Carlos Marques for critical reading of this manuscript. Simulation snapshots in this manuscript are rendered using VMD.[31]

References

1 H. G. Schild, M. Muthukumar and D. A. Tirrell, *Macromolecules*, 1991, **24**, 948.
2 G. Zhang and C. Wu, *Phys. Rev. Lett.*, 2001, **86**, 822.
3 J. Walter, J. Sehrt, J. Vrabec and H. J. Hasse, *J. Phys. Chem. B*, 2012, **116**, 5251.
4 H. Kojima, F. Tanaka, C. Scherzinger and W. Richtering, *J. Polym. Sci., Part B: Polym. Lett.*, 2012, **51**, 1100.
5 F. Tanaka, T. Koga and F. M. Winnik, *Phys. Rev. Lett.*, 2008, **101**, 028302.
6 D. Mukherji and K. Kremer, *Macromolecules*, 2013, **46**, 9158.
7 D. Mukherji, C. M. Marques and K. Kremer, *Nat. Commun.*, 2014, **5**, 4882.
8 M. A. Cohen-Stuart, W. T. S. Huck, J. Genzer, M. Müller, C. Ober, M. Stamm, G. B. Sukhorukov, I. Szleifer, V. V. Tsukruk,

M. Urban, F. Winnik, S. Zauscher, I. Luzinov and M. Minko, *Nat. Mater.*, 2010, **9**, 101.
9 M. A. Ward and T. K. Georgiou, *Polymers*, 2011, **3**, 1215.
10 S. de Beer, E. Kutnyanszky, P. M. Schön, G. J. Vancso and M. H. Müser, *Nat. Commun.*, 2014, **5**, 3781.
11 D. Mukherji, C. M. Marques, T. Stuehn and K. Kremer, *J. Chem. Phys.*, 2015, **142**, 114903.
12 C. H. Hofmann, S. Grobelny, M. Erlkamp, R. Winter and W. Richtering, *Polymer*, 2014, **55**, 2000.
13 S. Pronk, S. Pall, R. Schulz, P. Larsson, P. Bjelkmar, R. Apostolov, M. R. Shirts, J. C. Smith, P. M. Kasson, D. van der Spoel, B. Hess and E. Lindahl, *Bioinformatics*, 2013, **29**, 845.
14 W. F. van Gunsteren, S. R. Billeter, A. A. Eising, P. H. Hünenberger, P. Krüger, A. E. Mark, W. R. P. Scott and I. G. Tironi, *Hochschulverlag AG an der ETH Zürich*, 1996.
15 H. J. C. Berendsen, J. R. Grigera and T. P. Straatsma, *J. Phys. Chem.*, 1987, **91**, 6269.
16 J. C. G. Pereira, C. R. A. Catlow and G. D. Price, *J. Phys. Chem. A*, 2001, **105**, 1909.
17 H. J. C. Berendsen, J. P. M. Postma, W. F. van Gunsteren, A. DiNola and J. R. Haak, *J. Chem. Phys.*, 1984, **81**, 3684.
18 U. Essmann, L. Perera, M. L. Berkowitz, T. Darden, H. Lee and L. G. A. Pedersen, *J. Chem. Phys.*, 1995, **103**, 8577.
19 D. Mukherji, N. F. A. van der Vegt, K. Kremer and L. Delle Site, *J. Chem. Theory Comput.*, 2012, **8**, 375.
20 P.-G. de Gennes, *Scaling Concepts in Polymer Physics*, Cornell University Press, London, 1979.
21 J. Des Cloizeaux and G. Jannink, *Polymers in Solution: Their Modelling and Structure*, Clarendon Press, Oxford, 1990.
22 P. A. Netz, F. W. Starr, M. C. Barbosa and H. E. Stanley, *Physica A*, 2002, **314**, 470.
23 P. A. Netz, F. W. Starr, M. C. Barbosa and H. E. Stanley, *Braz. J. Phys.*, 2004, **34**, 24.
24 J. R. Kirkwood and F. P. Buff, *J. Chem. Phys.*, 1951, **19**, 774.
25 J. Rösgen, B. M. Pettitt and D. W. Bolen, *Biophys. J.*, 2005, **89**, 2988.
26 H. N. W. Lekkerkerker and R. Tuinier, *Colloids and the Depletion Interaction*, Clarendon Press, Oxford, 1990.
27 G. M. Torrie and J. P. Valleau, *J. Comp. Phys.*, 1977, **23**, 187.
28 B. Hess, H. Bekker, H. J. C. Berendsen and J. G. E. M. Fraaije, *J. Comput. Chem.*, 1997, **18**, 1463.
29 M. Sprik and G. Ciccoti, *J. Chem. Phys.*, 1998, **109**, 7737.
30 J. Kahlen, L. Salimi, M. Sulpizi, C. Peter and D. Donadio, *J. Phys. Chem. B*, 2014, **118**, 3960.
31 W. Humphrey, A. Dalke and K. Schulten, *J. Mol. Graphics*, 1996, **14**, 33.

